RESEARCH LABORATORIES
National Severe Storms Laboratory
Norman, Oklahoma
December 1967

Preliminary Quantitative Analysis Of Airborne Weather Radar

Technical Memorandum RLTM-NSSL 37

U.S. DEPARTMENT OF COMMERCE / ENVIRONMENTAL SCIENCE SERVICES ADMINISTRATION

U.S. DEPARTMENT OF COMMERCE
ENVIRONMENTAL SCIENCE SERVICES ADMINISTRATION
RESEARCH LABORATORIES

Research Laboratories Technical Memorandum- NSSL-37

PRELIMINARY QUANTITATIVE ANALYSIS OF AIRBORNE WEATHER RADAR

Lester P. Merritt

NATIONAL SEVERE STORMS LABORATORY
TECHNICAL MEMORANDUM NO. 37

NORMAN, OKLAHOMA
DECEMBER 1967

ENVIRONMENTAL SCIENCE SERVICES ADMINISTRATION

RESEARCH LABORATORIES

NATIONAL SEVERE STORMS LABORATORY TECHNICAL MEMORANDA

The National Severe Storms Laboratory, Norman, Oklahoma, in cooperation with other government groups, and with units of commerce and education, seeks to increase understanding of severe local storms, to improve methods for detecting these storms and for measuring associated meteorological parameters, and to promote the development and applications of weather radar.

Reports by the cooperating groups are printed as NSSL Technical Memoranda, a sub-series of the ESSA Technical Memorandum series, to facilitate prompt communication of information to vitally interested parties and to elicit their constructive comments. These Memoranda are not formal scientific publications.

The NSSL Technical Memoranda, beginning with No. 28, continue the sequence established by the U.S. Weather Bureau National Severe Storms Project, Kansas City, Missouri. Numbers 1-22 were designated NSSP Reports. Numbers 23-27 were NSSL Reports, and 24-27 appeared as a subseries of Weather Bureau Technical Notes.

Reports in this series are available from the Clearinghouse for Federal Scientific and Technical Information, U.S.Department of Commerce, Sills Bldg., Port Royal Road, Springfield, Virginia 22151.

LIST OF SYMBOLS

A	Area of a selected portion of a model storm
A_1	Area of the radar beam at range 1 n mi.
C	Constant which combines all the factors constant for a given weather radar system
D	Diameter of precipitation particles
G	Gain of the radar antenna
h	Radar pulse length in space
$\lvert K \rvert^2$	Dielectric constant for precipitation: $\lvert K \rvert^2 = 0.93$ for liquid water, 0.20 for ice
P_r, $\overline{P_r}$	Received echo power and its average value
P_t	Peak radar transmitter power
r	Precipitation rate
R	Distance from radar to target
U	Radar system losses
V	Transmission medium losses
W	Target loss
X	Radar beam orientation loss
Z	Radar reflectivity factor
Z_e	Radar reflectivity factor corresponding to Rayleigh scatterers returning the observed echo power
θ	Azimuthal beam width
λ	Wavelength
τ	Radar pulse length in time
σ	Radar (backscatter) cross section
η	Reflectivity
ψ	Composite attenuation function

ABSTRACT

Radar PPI photodata, obtained in a joint FAA/NSSL program utilizing FAA aircraft, an improved version of the Bendix RDR-1E airborne X-band radar, and the NSSL ground based Raytheon WSR-57 S-band radar, are compared within the framework of applicable radar theory. A simple theoretical model, simulating typical operation conditions, is developed in order to relate more clearly the expected performance of the airborne radar to that actually obtained in the test program. This model provides a basis for comparison of the ground and airborne radar data.

The analysis and data comparison is generally restricted to thunderstorms of only moderate intensity and size (rainfall rates $\leq$ 25 mm/hr; horizontal dimensions $\leq$ 8 n mi; vertical development $\leq$ 40,000 ft), and aircraft altitudes to 40,000 ft. Within these boundaries, however, agreement between the model, the airborne data, and the ground radar data is generally good.

The results indicate that the improved RDR-1E when operated under controlled conditions in the 10,000- to 40,000-ft altitude range with a grazing angle antenna tilt has the following approximate performance capabilities: (1) At altitudes between 30,000 and 40,000 ft, detection of moderate storms (rainfall rate$\simeq$25 mm/hr) at ranges of from 200 to 300 n mi, and storm system pattern identification at ranges from 125 to 175 n mi; (2) at altitudes of 20,000 to 30,000 ft, storm system pattern identification at ranges from 100 to 150 n mi, and reasonably good individual storm resolution in the range limits from 50 to 100 n mi; (3) at altitudes from 10,000 to 20,000 ft, storm system pattern identification at ranges from 75 to 125 n mi, and excellent individual storm resolution in the range limits from 20 to 70 n mi. Restrictions on and exceptions to these performance limits are discussed in some detail.

A simple computational technique is applied to the performance analysis of a particular airborne radar in meteorological situations of a rather special class. From the results, it would appear that a computer program could provide accurate estimates of radar performance for many potentially hazardous meteorological conditions. Such a program, applied to the wide range of radar types, flight modes (low altitude, high altitude, subsonic, supersonic, etc.), and meteorological conditions, would aid in resolving much of the controversy over optimum design characteristics, and provide urgently needed information relevant to flight safety in commercial, general, and military aviation.

TABLE OF CONTENTS

PRELIMINARY QUANTITATIVE ANALYSIS OF AIRBORNE WEATHER RADAR

Lester P. Merritt
National Severe Storms Laboratory

1. INTRODUCTION

The preliminary airborne phase of an FAA/NSSL radar comparison program was started in June 1966. As originally defined, the purpose of this study was to explore the feasibility of extending the range at which thunderstorms can be detected by appropriate modification of existing airborne systems and by wavelength selection.

Arrangements were made to equip aircraft based at the FAA Center, Oklahoma City, with the radar and recording instrumentation required, and to make them available, as needed, for flight tests. In addition, NSSL was committed to provide thunderstorm reflectivity data for all flights, and to direct flight operations to accomplish the test objectives.

Two specific types of flight tests were formulated:

(1) Maximum detection range test, wherein the aircraft would fly approach patterns at prescribed altitudes up to 40,000 ft, and in the range from 300 to less than 175 n mi from selected areas of storm activity. The selection of these areas would be based on their intensity and proximity to the NSSL radar.

(2) Penetration tests, wherein the aircraft would make close approach passes at selected areas of storm activity after completion of the maximum range tests on any given flight. In this way it was hoped that penetration (attenuation) data could be obtained to provide a measure of the absorption and scattering loss at X-band.

The operational phase of this program was conducted in July and August, 1966. Seasonally, this was a period of minimal convective activity in Oklahoma; thus, with rare exception, only light to moderate thunderstorms were encountered. The radar selected for this first study, an improved X-band RDR-1E, was initially installed in a CV880 and later transferred to an Electra II. Of the several flight tests conducted, most produced qualitatively significant data, and three produced data suitable for comparison with the NSSL WSR-57 radar. These three tests occurred, respectively, on July 29, July 30, the day prior to

removal of the CV880 from the program, and on August 13, with the radar installed in the Electra II. Of necessity, these cases must serve as the focal point of the discussions to follow. The reader is cautioned, however, that they are not representative of the severe storm systems for which improved radar capability is most urgently needed.

In order to present as objective a case as possible for both the positive and negative aspects of this experimental program it is appropriate to consider and evaluate the data within the context of the applicable radar theory. To this end a brief treatment of the radar equation is given, followed by a comparison of the characteristics of the RDR-1E and WSR-57 radars. A simplified radar-thunderstorm system model is then developed to demonstrate various aspects of the airborne radar problem and to obtain an estimate of performance limitations to be expected of the RDR-1E. From this framework the data collection program and results of the data comparison are considered. Although it was not possible to obtain data covering a wide range of important naturally occurring storms, it is hoped that this limited study is a useful first step forward development of a comprehensive guide for use of airborne weather radar.

2.0 THE RADAR EQUATION FOR METEOROLOGICAL ECHOES

2.1 Basic Equation

Starting with the basic radar equation (Kerr, 1951):

$$P_r = \left[\frac{P_t G^2 \lambda^2 \sigma}{(4\pi)^3 R^4}\right] \Psi \quad , \tag{1}$$

where the quantity Ψ is a composite attenuation function, the following assumptions are made: (1) The total radiated power is contained within the antenna beam angle defined by the half-power points; (2) the target consists of numerous scatterers distributed uniformly over the beam; (3) the radar wavelength is large compared with the dimensions of the scatterers; and (4) the attenuation function, Ψ, is taken as unity.

2.2 Volume Distribution and Reflectivity Factor

Based on assumptions 1 and 2, the radar (backscatter) cross section, σ, may be expressed in the form (Skolnik, 1962):

$$\sigma = V_m \eta = V_m \sum_i \sigma_i \quad , \tag{2}$$

where σ_i is the cross section of the i^{th} particle and V_m is the is the volume coverage of the antenna beam defined by the half-power beam angles and given by:

$$V_m = \frac{\pi}{4} R^2 \theta \phi \frac{h}{2} \quad . \tag{3}$$

Introducing the Rayleigh approximation (assumption 3) to Mie scattering theory (Gunn and East, 1954), (2) becomes:

$$\sigma = \frac{\pi^6 R^2 \theta \phi h |K|^2 \sum_i D_i^6}{8 \lambda^4} \quad , \tag{4}$$

where the quantity $\Sigma_i D_i^6$ (the summation of the sixth powers of particle diameters) is generally designated by the symbol Z and has been termed the reflectivity factor (Atlas, 1963) to avoid confusion with the reflectivity, η. Z corresponds to the rainfall rate, r, through the approximate relationships (Marshall and Palmer, 1948):

$$Z = \sum_i D_i^6 = 200 r^{1.6} \quad , \tag{5}$$

where units of Z are mm^6/m^3 and r is given in mm/hr.

Combining (1) through (5) under assumption (4) yields the radar equation for meteorological echoes:

$$\bar{P}_r = \frac{\pi^3 P_r G^2 \theta \phi h Z |K|^2}{512 R^2 \lambda^2} \quad , \tag{6}$$

where the bar implies averaging over many independent radar sweeps. This derivation applies when the distributed targets (precipitation particles) fill the whole beam volume defined by (3). Combining into a lumped constant, C, all the parameters of (6) that are essentially fixed for a given radar, we have

$$\bar{P}_r = \frac{Z |K|^2 C}{R^2} \quad . \tag{7}$$

Since the actual drop size distribution is unknown, and may extend beyond the Rayleigh region, it is necessary to define an equivalent reflectivity factor, Z_e, in order to use (7) quantitatively. Thus, Z_e is defined as the summation of a distribution (not necessarily specified) of Rayleigh scatterers, that would produce the signal power actually received. Based on this definition (7) may be expressed in the form:

$$Z_e = \frac{\bar{P}_r R^2}{|K|^2 C} \quad . \tag{8}$$

When Z_e is expressed in mm^6/m^3 with $\bar{P}_r$ in watts and R in nautical miles the constant C becomes:

$$C = 1.67 \times 10^{-23} \left[\frac{P_t G^2 \theta \phi \tau}{\lambda^2} \right] , \tag{9}$$

where the parameters are as follows:

P_t - transmitter power in watts

G - antenna gain

θ, ϕ - half-power beam widths in degrees

λ - radar wavelength in centimeters

τ - transmitter pulse width in microseconds

Equations (8) and (9) differ from those given by Wilk, et al. (1965) only by the retention of $/K/^2$ as a variable and the inclusion of P_t in the radar constant.

2.3 Applied Radar Equation

For the S-band WSR-57, as operated at NSSL, (7) is reasonably accurate within 100 n mi (Baxter, 1966). For an X-band airborne radar, however, such as the RDR-1E used in this investigation, the constraining assumptions upon which (7) is based are unrealistic.

For example, the target may fill only a fraction, f, of the beam volume. Then (3) becomes

$$V_m = \left[\frac{\pi}{4} R^2 \theta \phi \frac{h}{2} \right] f = \left[\frac{\pi}{4} R^2 \theta \phi \frac{h}{2} \right] \frac{R_e^2}{R^2} \quad . \tag{10}$$

where R_e is the range less than R at which the target just fills the beam. With this consideration and the attenuation term introduced in (1) taken into account, (7) becomes

$$\bar{P}_r = \frac{Z|K|^2 R_e^2 C \psi}{R^4} \quad . \tag{11}$$

The attenuation term, ψ, is a composite of all losses other than partial beam filling and may be expressed as:

$$\psi = 10^{-0.1(U+V+W+X)} \quad , \tag{12}$$

where the losses in decibels are given by:

U - the radar system loss

V - the transmission medium loss

W - the target loss

X - the beam orientation loss

Substituting (12) into (11) and expanding logarithmically one may express P_r as follows:

$$P_r(\text{dBm}) = 10(\log Z + \log|K|^2 + \log C) + 20 \log R_e - 40 \log R - (U+V+W+X) + 30 \quad , \tag{13}$$

where the numerical constant represents the conversion from dbw to dbm. The radar equation in this form is somewhat more useful for determining the performance limitations of weather radars in general and the RDR-1E in particular. Note that, although the factor X allows a correction for the assumption of constant antenna gain, no consideration has been given to the effects of side lobes.

3. ANALYSIS OF RADAR EQUATION PARAMETERS FOR THE WSR-57 AND THE RDR-1E

3.1 Relative Performance of WSR-57 and RDR-1E Radars without Special Losses

The performance characteristics for the WSR-57 and the RDR-1E are listed in table 1. Substituting the appropriate quantities from this table into (9) and taking the ratio of

Table 1 - RADAR CHARACTERISTICS

	WSR-57	RDR-1E	Improved RDR-1E
Wavelength	10 cm	3.2 cm	3.2 cm
Peak Power	400 kw	50.0 kw	50.0 kw
Antenna gain	38.3 db	34.5 db	34.5 db
Pulse length	4 sec	2.5 sec	5.5 sec
Minimum detectible Signal	-108 dbm	-102.0 dbm	106.5 dbm**
PRF	164 pps	400 pps	200 pps
Display range	250 n mi	180 n mi	300 n mi
Horizontal beam width Θ (half power)	2.0°	3°	3°
Vertical beam width ϕ	2.0°	3°	3°
Polarization	Linear	Linear	Linear
Antenna rpm	1*	15	15
Peak power in the first side lobe compared to the main lobe			
Azimuth	-20 db	-18 db	-18 db
Elevation	-20 db	-17 db	-17 db

*Variable
**Nominal measured value was 105 dbm

MDS (minimum detectable signal) power to C, yields a measure of the radar performance, $\frac{P_r(MDS)}{C}$:

Radar	C	$P_r(MDS)/C$
WSR-57	4.88×10^{-11}	3.5×10^{-4}
RDR-1E	4.0×10^{-11}	7.9×10^{-4}

Thus, all other factors being equal, the theoretical detection sensitivity of the WSR-57 is about 3.5 db greater, or slightly more than twice that of the RDR-1E. Usually, however, the parameters of (13) that are not included in (7) are not equal, but depend on several factors, such as radar wavelength and antenna beam width, geometry of the radar-target configuration, conditions in the transmission path, etc. These aspects are considered briefly below.

3.2 Vertical Profile of the Reflectivity Factor Z

Several vertical reflectivity factor profiles are given in figure 1. The shape of the profiles as a function of storm intensity is clearly shown. Special note should be taken of the classes of storms and their associated reflectivity maximums. The solid curve (Wilk, 1966) is a statistically weighted mean curve for Oklahoma and represents the spectrum shown by curves 1 through 4.

In general the storms under surveillance in this study were of the convective thunder shower class given by profile 1. The maximum reflectivity factor rarely exceeded $10^{4.5} mm^6/m^3$, and dropped sharply at altitudes above 15,000 ft. For such storms, occurring within the normal operating range of the NSSL WSR-57 (20-100 n mi), the observed Z would be nearly maximized for 0° antenna tilt. For the RDR-1E, however, the value of Z observed depends greatly on aircraft altitude, antenna elevation, and range. The significance of the reflectivity factor distributions for storm detection at great ranges is considered in sections 4 and 6 below.

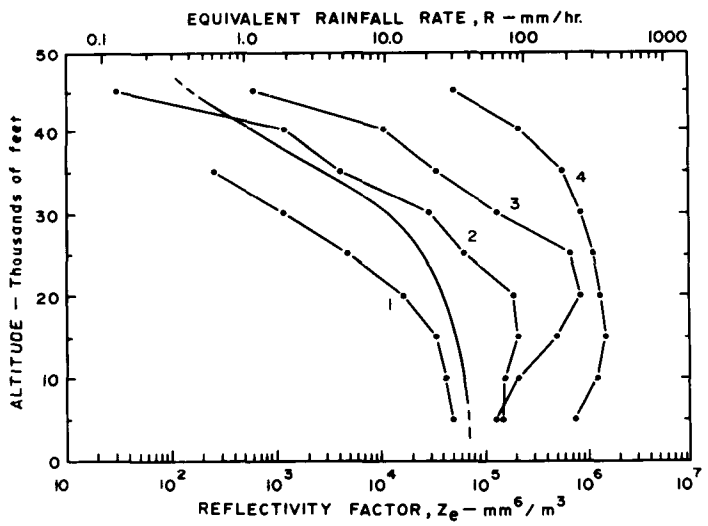

Figure 1. Median vertical reflectivity factor profiles for various classes of convective storms. Curves 1, 2, and 3 were obtained by Donaldson (1961) with a 3.2-cm CPS-9 in New England, and curve 4 by Inman and Arnold (1961) with a CPS-9 in Texas. The classes of storms represented by these curves are as follows: 1. thundershower; 2. hail storm; 3. tornadic storm; 4. tornadic storm. The solid curve (Wilk, 1966) represents a statistical average of Oklahoma storms spanning the range indicated by curves 1 through 4.

3.3 The Dielectric Parameter $/K/^2$

The parameter $/K/^2$ has the value of 0.93 for liquid water and 0.20 for ice. In terms of (13) the difference represents 6.8 db of received power. For normal ground radar operation, the value for liquid water is usually taken, but when the radar illuminates ice in the upper portion of storms, or a mixture of ice and water particles, the back scatter loss associated with low $/K/^2$ should be treated. This is a complicated matter, because ice with a wet outer surface may scatter like pure water (Atlas, 1963). The effects of ice should, however, be considered in the case of airborne radar at high altitudes and great ranges.

3.4 The Effective Beam-Filling Range, R_e

The value of R_e depends on the physical dimensions of the target storm, the altitude of the radar with respect to the storm, and the beam width and orientation of the antenna. The approximate value of R_e for the WSR-57 (as operated at NSSL) was determined from a statistical study to be about 80 n mi (Baxter, 1966). In other words, for most storms occurring within 80 n mi of NSSL, $R_e = R$, and effects of range on received power are well represented by the R^{-2} relationship. Under identical operating conditions, and on the basis of beam width considerations only, the beam-filling range of the RDR-1E is about 50 n mi. This may be observed from a consideration of the tangential beam widths given as a function of range in table 2. Depending on actual

Table 2 - ANTENNA RESOLUTION CHARACTERISTICS

	WSR-57				RDR-1E			
Range (n mi)	Tangential beam width		Cross-Sectional area of beam		Tangential beam width		Cross-Sectional area of beam	
	n mi	km	n mi^2	km^2	n mi	km	n mi^2	km^2
1	0.035	0.065	0.96×10^{-3}	0.33×10^{-2}	0.052	0.096	2.1×10^{-3}	7.2×10^{-3}
20	0.7	1.3	0.385	1.32	1.04	1.92	0.85	2.89
40	1.4	2.6	1.54	5.3	2.08	3.8	3.4	11.5
60	2.1	3.9	3.47	11.9	3.12	5.8	7.6	26.0
80	2.8	5.2	6.2	21.3	4.16	7.7	13.6	46.0
100	3.5	6.5	9.6	28.1	5.20	9.6	21.2	72.1
150	5.25	9.7	21.6	74.0	7.8	14.4	47.9	162.1
200	7.0	12.9	38.5	132.	10.4	19.2	85.0	290.
250	8.75	16.1	60.	206.	13.0	24.0	132.	415.
300	10.5	19.4	87.	297.	15.6	28.8	192.	608.

operating conditions (altitude, attitude, and radar and storm characteristics, etc.) however, the effective beam-filling range may be substantially less or greater.

3.5 Losses

The radar system loss, U, for the WSR-57, is essentially accounted for by measuring the system MDS rather than simply the receiver MDS. Unfortunately, no such measurement capability was available for the RDR-1E aircraft installation. Realistic losses therefore have been estimated as follows:

TR, waveguide, rotary joint and radome	2 db
Receiver, indicator, and photographic	2 db
Field degradation	3 db

Skolnik (1963) discusses these losses in detail. Two additional system losses, which may be neglected at beam-filling ranges but which become increasingly important at extended ranges, are those resulting from beam shape and scan rate. These are noted below in conjunction with orientation loss, X, and are discussed in section 4 in conjunction with maximum detection range limitations.

The transmission medium loss, V, is fundamentally dependent on radar wavelength, and conditions in the medium intervening between the radar and target. For the S-band WSR-57, V is essentially negligible over the range of meteorologically important conditions, but for the X-band RDR-1E it is highly variable and can range from negligible values in clear air to excessive ones in heavy precipitation. Values of V (in db/km) are given in table 3 for various weather conditions. A discussion of these losses is given in the specified source papers.

The target loss, W, is of the same character as the transmission medium loss, except that in this case its effect on target resolution and identification must be considered. For example, an increase in reflectivity factor, Z, from $10^{4.5}$ to $10^{5.5}$ results in an increase in attenuation from 0.6 to 5.49 db/km at a wavelength of 3 cm (Medhurst, 1965). Thus, the gain in signal strength from the increased reflectivity factor is fully canceled by attenuation after 1 km of penetration. The implication of verisimilitude, as pointed out in the McGill report (Marshall, et al, 1965) is quite clear. This point, in conjunction with the limitations of this investigation, is discussed in sections 6 and 7.

The beam orientation loss, X, depends on where in the beam the target storm is located. At the center of the beam, X is zero. At extended ranges, however, the center of the target region occupies an increasingly smaller portion of the beam cross section and may be appreciably away from the center of the beam, even at the point of closest approach. For conditions of

close approach of the target storm to the beam center, X is given by the Gaussian function:

$$X = -10 \log \left\{ \exp \left[5.55 \left(\frac{\theta_r}{\theta_B} \right)^2 \right] \right\} , \qquad (14)$$

where θ_r and θ_B are the radial and beam width angles respectively. The exponential expression in (14) is actually the beam shape loss for a conical beam. Using this equation, it is possible to subdivide the region of the beam occupied by the target into areas of approximately constant reflectivity factor and to compute position loss (section 4). Note that (14) applies only to the region within the half-power beam width; outside, the effects of side lobes are much more complicated, but are generally small enough to be neglected. Note also that the equation does not account for effects that arise from averaging the target hits over the beam and from antenna movement between pulses. A half-power beam cross section is given in figure 2. The concentric circles are marked both in degrees from zero center, and in db of beam shape loss from 0 at 0° to -6 db at the half-power beam width.

Table 3 - TRANSMISSION MEDIUM AND TARGET ATTENUATION (λ = 3 cm)

Condition	Precipitation rate (mm/hr)	Reflectivity factor* (mm^6/m^3)	Attenuation (db/km)
Clear air	0	0	Negligible
Ice cloud	0	0	$5.23 \times 10^{-4} M$ (T = -20°C)**
Water cloud	0	0	$11.2 \times 10^{-3} M$ (T = -8°C)
Light rain	0 to 5	0 to $10^{3.4}$	0 to 0.718×10^{-1}***
Medium rain	5 to 25	$10^{3.4}$ to $10^{4.5}$	0.718×10^{-1} to 0.6
Heavy rain	25 to 150	$10^{4.5}$ to $10^{5.8}$	0.6 to 5.49
Very heavy rain	Over 150	Over $10^{5.8}$	Over 5.49

* Based on Marshall and Palmer (1948) relationship.

** After Gunn and East (1954) - M in g m^{-3}.

*** After Medhurst (1965).